Hindawi
Geofluids
Volume 2024, Article ID 6631646, 12 pages
https://doi.org/10.1155/2024/6631646

Research Article

Stability Analysis of Retaining Wall in Backfilled Stope Based on Catastrophe Theory and Numerical Analysis

Chang Liu[1,2] **Kui Zhao**[1,2,3] **Peng Zeng**[1,2,3] **Cong Gong**[1,2] **Liangfeng Xiong**[1,2] **Jinbo Xiong**[4] **and Rongsen Pan**[4]

[1]*College of Resources and Environmental Engineering, Jiangxi University of Science and Technology, Ganzhou, Jiangxi 341000, China*
[2]*Jiangxi Provincial Key Laboratory of Low-Carbon Processing and Utilization of Strategic Metal Mineral Resources, Ganzhou, Jiangxi 341000, China*
[3]*Jiangxi Provincial Key Laboratory of Safe and Efficient Mining of Rare Metal Resources, Ganzhou, Jiangxi 341000, China*
[4]*Yongping Copper Mine, Jiangxi Copper Corporation Limited, Shangrao, Jiangxi 334506, China*

Correspondence should be addressed to Peng Zeng; zengpeng@jxust.edu.cn

Received 14 June 2023; Revised 24 March 2024; Accepted 28 March 2024; Published 18 April 2024

Academic Editor: Dan Ma

Retaining wall is essential for stopes mining in two steps, for it can prevent the instability and collapse of backfill. In this study, taking the retaining wall of backfilled stope as the research object, a stability analysis method of retaining wall based on the close coupling of catastrophe theory and numerical analysis was proposed. First, by extracting the unit failure rate of the retaining wall from the numerical simulation results and fitting it with the mining depth, the functional expression between them was established. Second, the function relation was transformed into the normal form according to catastrophe theory, and the instability criterion of retaining wall was deduced. Furthermore, an effort was made to analyze the changing law of the state of retaining wall and calculate the critical span of stope, under different thickness conditions. On this basis, the application test of retaining wall was carried out by using this method. The results show that with the thickness decreasing, the values of splitting variables a and b show a reverse trend, which leads to the discriminant of instability criterion decreasing and turning from positive to negative, resulting in the collapse. Meanwhile, in order to ensure the stability, the wider the span of the stope, the thicker the retaining wall is required, and conversely, the thicker the retaining wall, the higher the adaptability to the span of stope. In addition, it can be found from the application test that instability was bound to occur with a thickness of 3 m, but the retaining wall with a thickness of 4 m maintained stable, which tended to be consistent with the analysis. Therefore, the stability analysis method proposed in this study provides a way to accurately evaluate the stability of the retaining wall and calculate the critical thickness of that, and its application value is expected to be further explored.

1. Introduction

Due to its low strength and poor integrity, backfill is often a relatively weak part of the mining system [1–3]. For stopes mined in two steps, the disturbance of the backfill in the first-step stope caused by the second-step mining is inevitable [4, 5]. Given that the backfill in the first-step stope is unstable and easy to collapse, the second-step mining is beset with difficulties [6, 7] (Figure 1(c)). Therefore, the original orebody with a certain thickness is reserved outside of the backfill, which becomes a solid "shell," namely, the retaining wall (Figure 1(a)). The stability of the retaining wall is related to that of the backfill, which is also the external barrier that ensures the stability of backfill, the key to maintain mining filling balance, and the premise of safe and efficient mining (Figure 1(b)).

As a support structure, the retaining wall can be regarded as a special pillar. For a long time, there are few researches on retaining wall around the world, and similar researches on pillar stability are mostly based on empirical

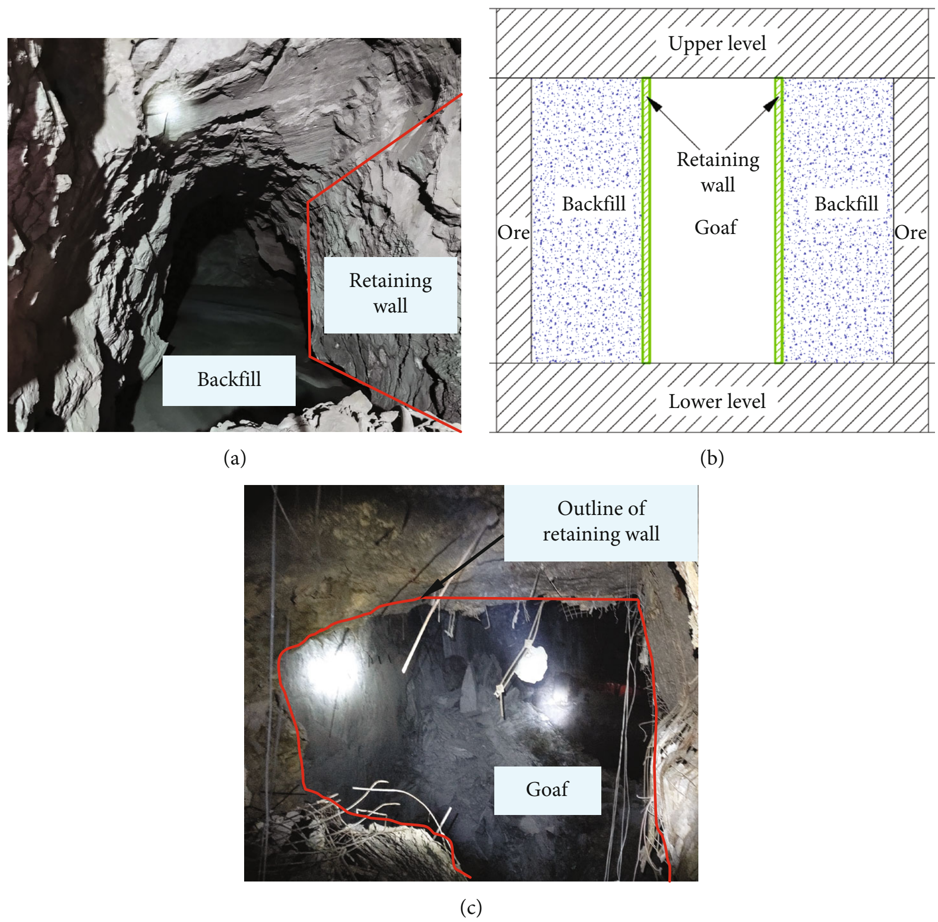

Figure 1: Position of retaining wall, goaf, and backfill: (a) intact retaining wall, (b) the spatial position of retaining wall, and (c) collapsed retaining wall.

formula, theoretical calculation, similar simulation, and numerical analysis [8–13]. As part of the bearing structure, the stress concentration gradually appears when the thickness decreases [14, 15], and the continuous reduction of the thickness can eventually cause its destruction. However, if the roof and the pillar are considered as an integral support system, the stability of the support system is jointly controlled by the stope structural parameters, the overlying load, and the lateral pressure of the backfill [16, 17]. By comprehensively analyzing the factors affecting and establishing the pillar stability calculation formula containing multiple factors, it will certainly help to determine whether the pillar is destabilized and to deduce the safety factor and minimum size of the pillar.

In addition, as a mathematical method, catastrophe theory is widely used in stability evaluation, instability prediction, and risk assessment of various types of projects [18–21]. In underground engineering research, catastrophe theory can be used to establish destabilization criteria for tunnels, chambers, or mining areas, which is a way to explore the instability mechanism of underground space [22–25]. According to a series of previous studies, it is clear that the key to the engineering application of mutation theory is to accurately establish relational expressions that reflect the equilibrium state [26–28]. However, as a special type of pillar, the retaining wall is located in an extremely complex mechanical environment, which makes it very difficult to derive the instability criterion directly using the catastrophe theory, and as a result, most of the retaining wall stability studies using catastrophe theory end up in the dilemma of equation derivation.

In conclusion, a series of researches have made numerous achievements in stability analysis of pillar, instability failure mechanism [29, 30], safe size calculation, etc., but research on retaining wall of filling stope is extremely rare. In this study, a mathematical model between mining depth and unit failure rate of retaining wall is established by combining catastrophe theory with numerical simulation. The unit failure rate increases with continuous decrease of the thickness of retaining wall until the instability and failure occurs. Then, the critical thickness of retaining wall can be accurately calculated. This provides a brand-new method for the study of retaining wall stability.

2. Thickness Reduction Method for Retaining Wall

2.1. Instability Criterion of Catastrophe Theory of Retaining Wall. According to the catastrophe theory, the state of mechanical system can be expressed by the mathematical function relation composed of several parameters [31, 32].

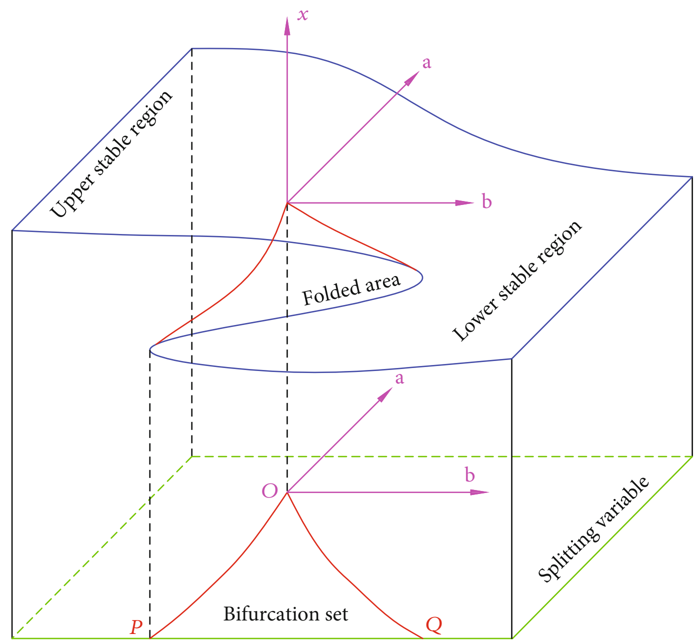

Figure 2: Relation of elements in cusp catastrophe model.

$$y(x) = x^4 + ax^2 + bx. \quad (1)$$

Equation (1) is the standard expression of catastrophe, in which x is the status variable and a and b are the splitting variables.

Derive equation (1) and make it equal to 0; then,

$$x^3 + ax + b = 0. \quad (2)$$

Equation (2) is the equilibrium surface equation of equation (1), and its corresponding geometric shape is a surface, which composed of the upper stable region, the folded area, and the lower stable region [33, 34], as shown in Figure 2. According to the cusp catastrophe theory, both the lower stable region and the upper stable region of the surface stand for the stable state, while the folded area is in the mutation stage, which stands for the unstable state [35, 36]. The state of the system can be described by the motion of a point on the equilibrium surface. There are thousands of transition paths of the point, and each path represents one state of the system. However, no matter what path it is, the system will become catastrophic unstable as long as it enters the folded area. The equilibrium surface and its elements are projected on Figure 2, and a bifurcation set with POQ as the end point is formed on the splitting variable plane. Only when the splitting variable passes through the bifurcation set from left to right, the stable state of the system is broken and catastrophic instability occurs [37, 38].

The criterion for instability of the system can be expressed in the form of mathematical expression, that is,

$$\begin{cases} a < 0, \\ 8a^3 + 27b^2 < 0. \end{cases} \quad (3)$$

When the equilibrium equation (2) meets the requirements of equation (3), the system is unstable. Regard the retaining wall as a system and the thickness as the influencing factor of the splitting variable. The state of the wall will change suddenly when the thickness of the wall, which continuously reduces, is at a certain value. According to the catastrophe theory, catastrophic instability will occur in the system when equation (3) is satisfied, which means that the retaining wall is collapsed. Therefore, it is a good method to evaluate the stability of the retaining wall through applying catastrophe theory to analyze the state in the process of wall thickness reduction.

2.2. Instability Analysis Method of Retaining Wall Based on Catastrophe Theory and Numerical Analysis. The catastrophe theory and numerical analysis are used to analyze the instability of retaining wall. The basic principles are as follows: first, the unit failure rate of retaining wall at different mining depth can be obtained by numerical simulation analysis; second, the wall stability analysis model with the coupling of catastrophe theory and numerical analysis can be obtained by fitting the unit failure rate with the normal form of catastrophic model; third, the mathematical expression of retaining wall instability can be obtained by deducing its criterion; fourth, a list of equilibrium equations can be obtained by continuously reducing the thickness of retaining wall to promote the transition from stable state to unstable state; and finally, these equilibrium equations can be analyzed to ascertain whether they meet the criterion for instability or not, and the thickness of retaining wall in the critical state—the catastrophic instability suddenly occurs—can be calculated.

The effect of thickness on stability can be found by closely combining catastrophe theory and numerical analysis. The main steps are as follows.

Regard the original thickness of retaining wall as A_0 and the common difference as d, and reduce the same thickness of retaining wall every time. After i times of reduction, the thickness is A_i; then,

$$A_i = A_0 - id. \tag{4}$$

A numerical model of stability analysis of retaining wall with the original thickness A_0 is established to simulate mining at different depths, extract the number of retaining wall failure units, and calculate the unit failure rate at different depth of mining.

$$k_x = \frac{n_x}{N_x}, \tag{5}$$

where k_x stands for the unit failure rate at the depth of x and n_x and N_x stand for the amount of failure units and the total number of retaining wall units, respectively.

Reduce the thickness of retaining wall and then establish the numerical model of retaining wall with the thickness of A_i. By doing so, mining can be simulated to get the number of retaining wall failure units and calculate the unit failure rate with different thickness:

$$e_i = f(x, A)\frac{m_i}{M_i}, \tag{6}$$

where e_i denote the unit failure rate of retaining wall after i times of thickness reduction. In addition, m_i and M_i stand for the amount of the retaining wall failure units with the thickness of Ai and the total number of retaining wall units, respectively.

Fit equation (6) by applying the quartic equation with one unknown, and then, the function containing the unit failure rate of the retaining wall, which changes with the depth x and thickness A, can be obtained as follows:

$$e = f_1(A)x^4 + f_2(A)x^2 + f_3(A)x, \tag{7}$$

where $f_1(A)$, $f_2(A)$, and $f_3(A)$ are all functions related to the thickness A.

Analyze equation (7) and make

$$V = \frac{e}{f_1(A)}. \tag{8}$$

Thus, equation (7) can be written in the normal form of catastrophic model; then, get

$$V = x^4 + ax^2 + bx. \tag{9}$$

a and b in equation (9) are both functions related to the thickness A, in which

$$\begin{cases} a = \dfrac{f_2(A)}{f_1(A)}, \\ b = \dfrac{f_3(A)}{f_1(A)}. \end{cases} \tag{10}$$

Consequently, the traditional complex formula derivation method applied in mechanics analysis did not utilized in this study. Instead, the catastrophe theory and numerical analysis are combined for mathematical simulation method. By doing so, a and b in equation (10) can be obtained and substituted into equation (3) to determine whether the retaining wall is stable or not.

2.3. Analysis on Retaining Wall Thickness Reduction. To make the results of the study close to reality, a copper mine with its orebody orientation of about 1500 m, dip direction of 1200 m, dip of 70°~80°, and standard mining altitude of 100 m~1000 m is selected as the research object. *VCR* mining method is applied in this study, setting the stope height (h) of 50 m and the stope width (D) of 18 m. Mining is carried out in two steps, namely, the first-step mining and the second-step mining. The retaining wall of a certain thickness is reserved in the process of the first-step mining; after that, the goaf is backfilled with the backfill. And the second-step mining is carried out in the whole process of filling. A 3D numerical model (Figure 3) is established according to the technical parameters shown in Table 1. It should be noted that the unit failure rate is related to the shape and number of elements. To ensure the accuracy of simulation, the established model must have a unified scale; that is, all retaining walls are divided into grids using the same shape and size of elements. In addition, the mining and filling sequence of the numerical simulation is shown in Figure 4.

The original thickness (B) of the retaining wall is 8 m, which is reduced by 1 m at a time until its thickness is 2 m. The numerical simulation is carried out every time when the thickness is reduced. And the amount of the retaining wall failure units can be extracted to analyze the unit failure rate of retaining wall at different depth of mining. Consequently, a series of fitting curves can be obtained with the help of equation (9).

The fitting curves with retaining wall thicknesses of 8 m, 6 m, 4 m, and 2 m are shown in Figure 5. It is easy to find in the figure that the fitting curve is very smooth with no obvious inflection point and the maximum unit failure rate is only 28% when the thickness of the retaining wall is 8 m. However, the fitting curve is flat at first and then becomes steep when the thickness of the retaining wall is reduced to 2 m. Especially when the mining depth increases to 800 m, the curve almost changes from horizontal to vertical, and the maximum unit failure rate is up to 90%. Generally speaking, the thickness reduction will lead to the increase of the unit failure rate of retaining wall, and the fitting curve will change from flat to steep.

To facilitate the subsequent analysis, a new discriminant Δ is proposed, and let $\Delta = 8a^3 + 27b^2$. The values of the splitting variables a and b can be obtained by transforming the fitting curve into the mathematical expression. Each

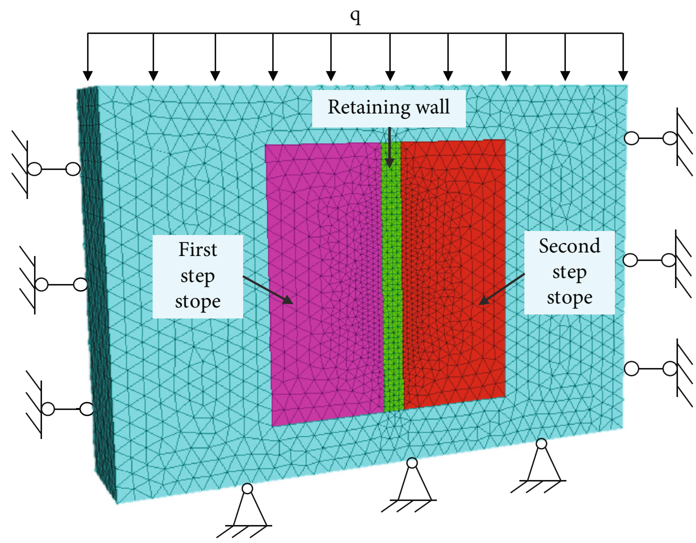

Figure 3: 3D numerical model.

Table 1: Mechanics parameters of ore and backfill.

Medium	Elastic modulus (GPa)	Poisson's ratio	Cohesion (MPa)	Friction (°)	Density (kNm^{-3})
Ore	21.2	0.25	6.8	27.5	34.3
Backfill	1.7	0.19	0.6	25.7	21.3

thickness reduction of the retaining wall produces the related value of a and b, from which a list of Δ values is obtained, as shown in Table 2.

With the reduction of the thickness of retaining wall, the fitting curve will continue to move upward. As a result, the splitting variables a and b, as well as the discriminant Δ, will change, as shown in Figure 6. The basic relationship between Δ and the thickness of retaining wall is that Δ decreases with the thickness reduction. When the thickness of retaining wall is reduced to 3 m, Δ will be less than 0 and the retaining wall will be unstable.

Therefore, the catastrophe theory is closely combined with the numerical analysis. The result of numerical analysis is used to establish catastrophe model through mathematical method. In addition, the instability criterion was deduced for analyzing the stability l, which is a new way to study the stability of retaining wall.

3. Analysis on the Adaptability of Retaining Wall to the Change of Stope Span

Similarly, the thickness of retaining wall (B) is still regarded as the fixed value, and stope width (D) is regarded as the variable. Increase the stope width from 10 m to 30 m, and the effect of span change on the stability of retaining wall can be analyzed. The unit failure rate is calculated whenever the stope width increases by 2 m, and a list of data can be obtained. Fit these data, and then, the variation curve of unit failure rate can be obtained.

The unit failure rate of retaining wall is positively correlated with the stope span; that is, the plastic zone in retaining wall increases with the increase of the span. Figure 7 shows the fitting curve with $B = 4$. When the stope span (D) is 10 m long, the failure rate is the smallest and the fitting curve is the red one at the bottom of all curves in the figure. In addition, the failure rate will increase with the increase of stope width (D), which will consequently lead to the rise of the position of fitting curves. When $D = 30$ m, the minimum unit failure rate of retaining wall is more than 40%, and the maximum of that is nearly 95%.

Curves, each of which correspond to a set of a and b, in Figure 7 are fitted by equation (9). Several fitting curves generated based on the numerical simulation results lead to the occurrence of a series of a, b, and Δ, as shown in Figure 8. The original thickness, span, and Δ value of the retaining wall are 4 m, 10 m, and 3.33, respectively. The Δ value will decrease with the increase of span, and the Δ value is -0.04 when the span increases to 22 m, which means that the catastrophic instability occurs according to discriminant (3). For this reason, 22 m is the critical span, namely, the span (D) should be less than 22 m to make the retaining wall ($B = 4$) stable. Similarly, the critical spans are obtained when the thickness of the retaining wall is 2 m, 3 m, and 5 m, respectively, which are 15 m, 18 m, and 28 m. When the retaining wall is thicker than 5 m, the critical spans are more than 30 m; that is to say, the retaining wall will be stable as long as the span is less than 30 m. It can be seen that the thicker the retaining wall is, the better the adaptability of the stope is to the span.

The numerical simulation results can also directly explain the instability process of retaining wall. From the transformation process of the plastic zone, the state of

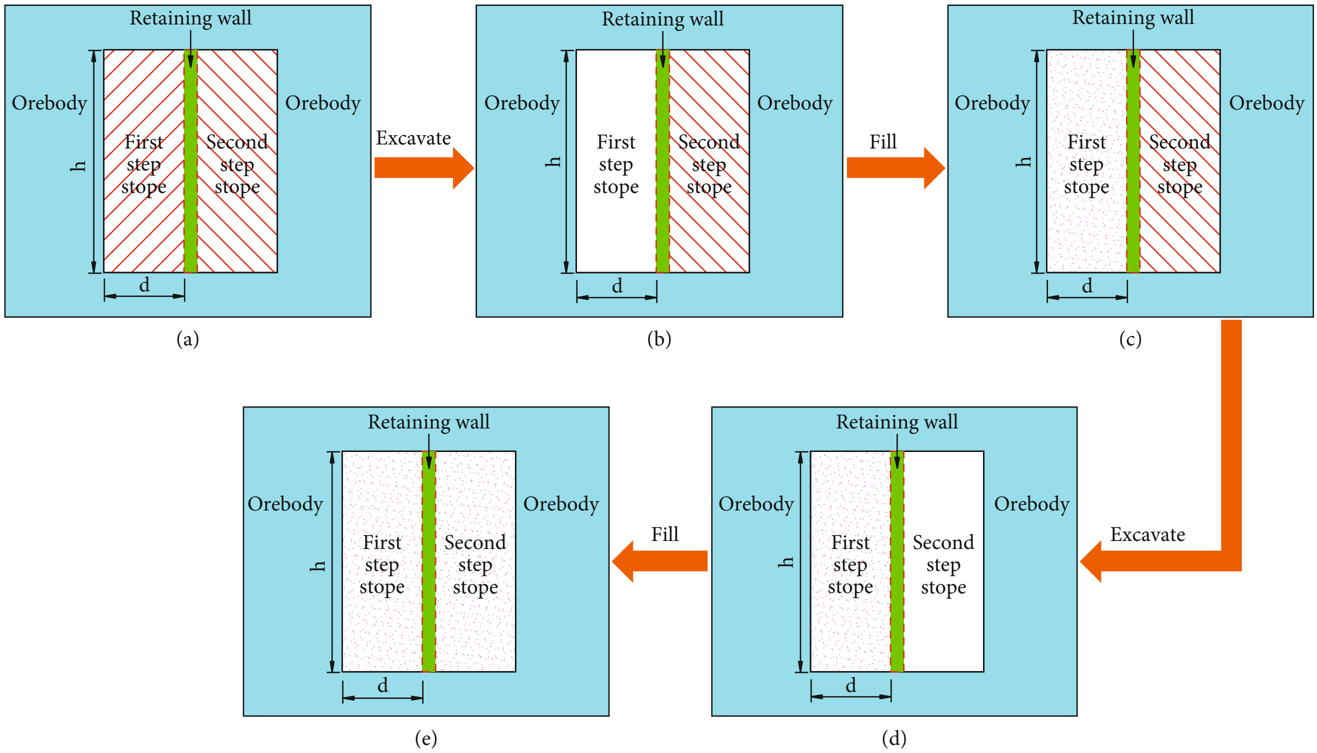

FIGURE 4: Mining and filling sequence of the numerical simulation: (a) initial state, (b) first-step mining, (c) first-step filling, (d) second-step mining, and (e) second-step filling.

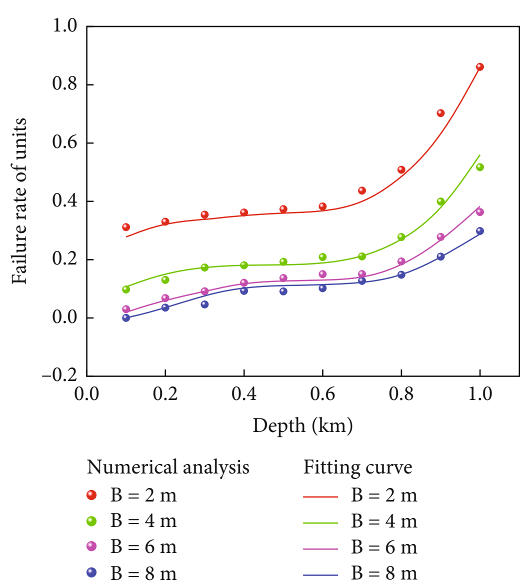

FIGURE 5: Unit failure rate of retaining wall at different mining depth.

retaining wall can be divided into three states, namely, stable state, critical state, and unstable state. Figure 9 shows the evolution of the plastic zone of the wall, which has a thickness of 4 m and is located at a depth of 1000 m. In the course of the stope span increasing from 10 m to 20 m, which refers to the stable state, the retaining wall can adapt well; thus, the plastic zone is only scattered with the failure rate less than 30%. When the span is larger than 20 m, which means that the retaining wall enters the critical state, the plastic zone expands rapidly and the scattered plastic elements gather together, thus making the plastic zone develops from one point to an area and the unit failure rate more than 40%. If the span continues to be increased, the number of failure units will increase sharply, which will lead to the interconnection between the plastic zones. By doing so, the retaining wall will be destroyed by the plastic zone, and the failure rate can reach 60%. Obviously, with the increase of the span, the stability of retaining wall tends to be worse [39], and the retaining wall will go from stable to unstable.

4. Application of Retaining Wall

To verify the research results, the application test of retaining wall was carried out in stope #2 at 550 m level of the copper mine. The buried depth of stope #2 is about 800 m, and the span of it is 18 m. There is backfill on both sides of stope #2 during mining, for the stope is between stope #1 and stope #3. To successfully carry out the research, the retaining wall with the thickness of 3 m and 4 m is designed on both sides of stope #2, respectively. Besides, the goaf is scanned after mining to obtain the exact shape of it.

According to the scanning results of the goaf (Figure 10(b)), it can be known that the stability of retaining walls with different thickness is quite different. In terms of the retaining wall with a thickness of 3 m, a massive collapse occurred in the middle and upper parts of the retaining wall (Figure 10(a)), and the collapsed part fell into the backfill in stope #1. On the contrary, the main body of the retaining

Table 2: State of retaining wall with different thickness.

Retaining wall thickness (m)	Splitting variable a	Δ	State
8	-2.12	2.91	Stable
7	-1.96	2.28	Stable
6	-1.81	1.98	Stable
5	-1.66	1.57	Stable
4	-1.28	0.93	Stable
3	-0.99	-0.03	Unstable
2	-0.80	-0.59	Unstable

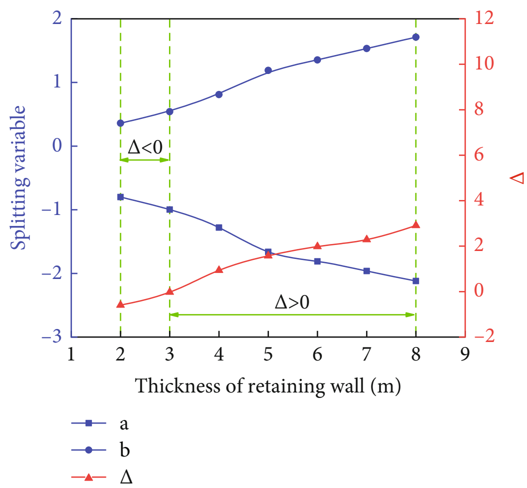

Figure 6: Variation of a, b, and Δ with B.

wall with a thickness of 4 m does not change significantly (Figure 10(c)) but only caves slightly. As a result, it fully shows the protection of retaining wall to the backfill.

In the course of mining, through continuous observation of the extracting drift at the bottom of stopes (Figure 11(b)), it is found that there are only broken blocks in extracting drift of stope #3, while there are a large number of filling mass in that of stope #1 (Figure 11(c)). Therefore, it can be known that the retaining wall with a thickness of 3 m is bound to collapse. Moreover, in the drilling chamber at the top of stopes, the retaining wall with a thickness of 3 m collapsed on a large scale, while the retaining wall with a thickness of 4 m still remains stable and stands safely between the stopes (Figure 11(a)).

According to the application test results of retaining wall, the stability of retaining wall can be accurately evaluated by the criterion of catastrophic instability, which is established by closely combining catastrophe theory with numerical analysis. The research results are instructive, for they can guide mining very well, which can realize the smooth and orderly connection of the first-step mining and the second-step mining.

5. Discussion

5.1. Application of Catastrophe Theory. Catastrophe theory is in essence a mathematical method that is commonly utilized to study rock mass instability. In the field of underground

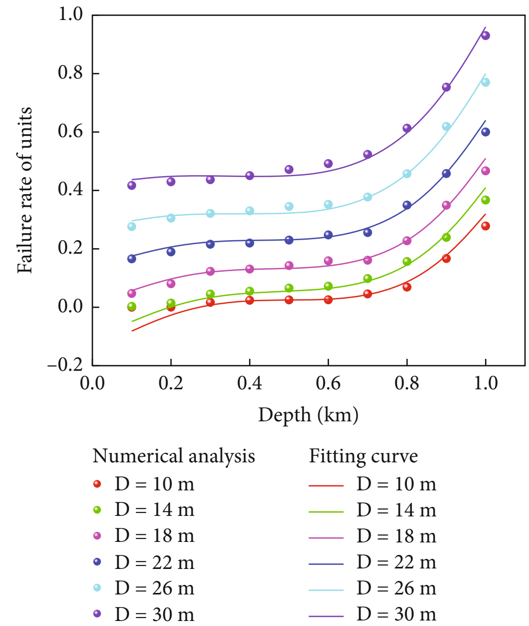

Figure 7: Fitting curves at different stope spans.

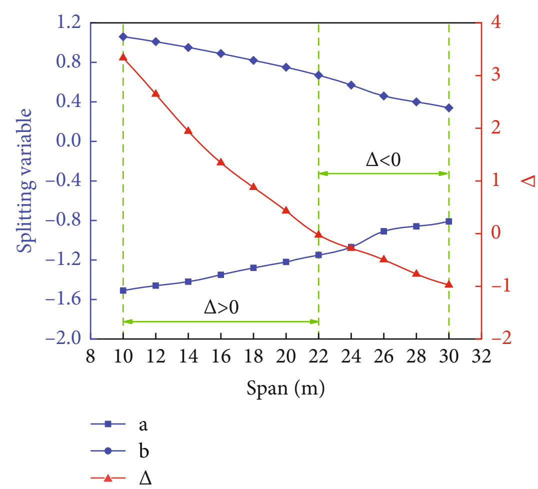

Figure 8: Variation of a, b, and Δ with D.

engineering, the catastrophe theory has played a unique role in the study of state changes of support structures, especially the destabilization of mine pillars and roof [40–42]. Located between the backfill and the rock mass, the retaining wall is in a very complex mechanical environment, and its state change is influenced by many factors. So far, most of the studies are based on qualitative evaluation, and researchers rarely studied the stability of retaining wall by catastrophe theory. In view of this, this study introduces the catastrophe theory into the study of retaining wall stability in the filling stope and deduces the development process from stability to instability by continuously reducing the thickness, which provides a new idea for quantitative analysis of retaining wall stability.

The key to the application of the catastrophe theory is to establish the catastrophe model and derive the catastrophe instability criterion. Most of the traditional research methods are very tedious and prone to errors, because they

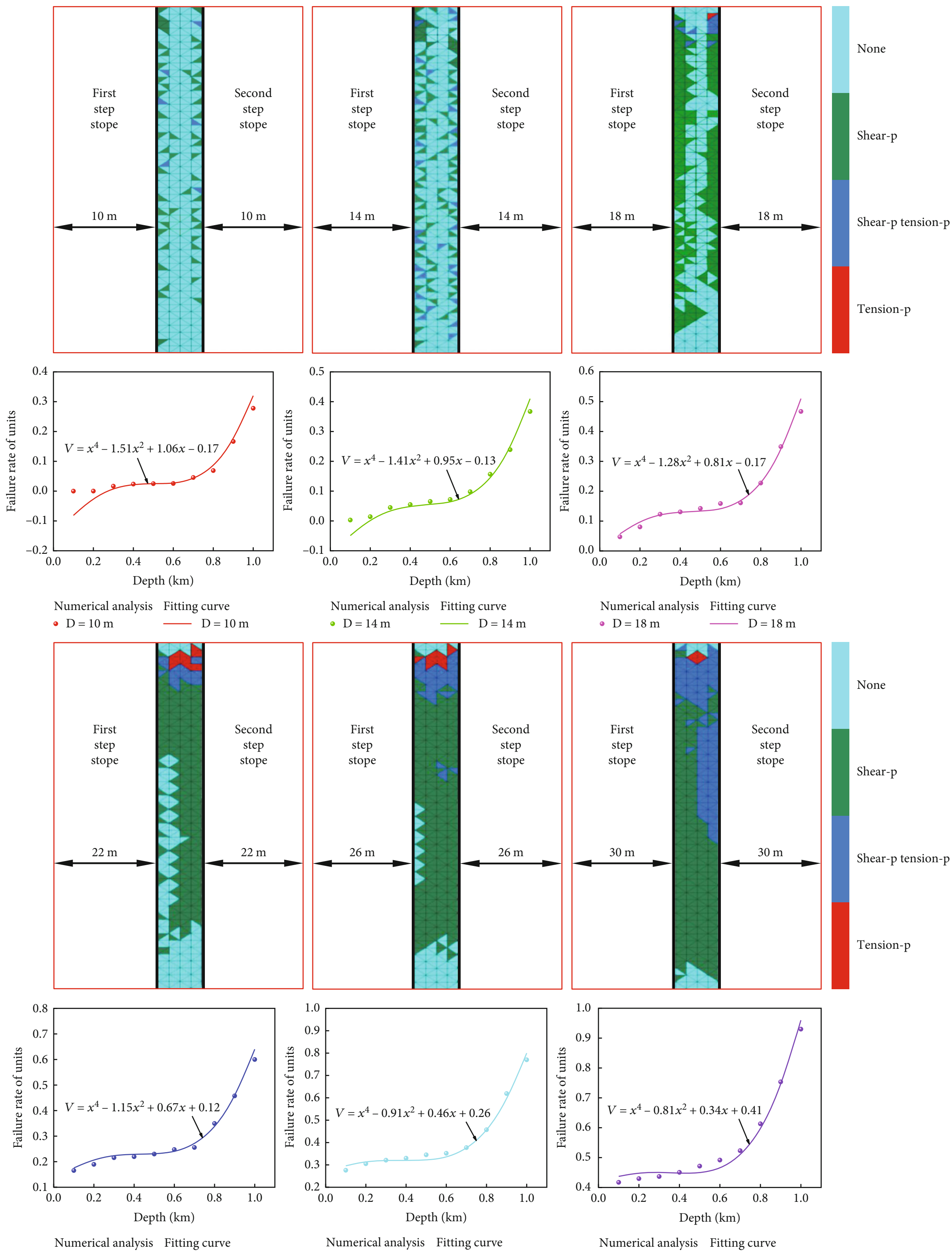

Figure 9: Distribution of plastic zone in retaining wall with different spans.

begin with the force of the analytical object and the standard expression of catastrophe model is established through numerous mathematical formula derivation and relational conversion. In this study, the numerical simulation analysis is used to obtain the unit failure rate of retaining wall under different mining depth conditions, and the unit failure rate is fitted in the form of catastrophe theory standard to establish the standard expression of catastrophe. On the basis of this derivation, the criterion of retaining wall instability was obtained. Without complex formula derivation, the method

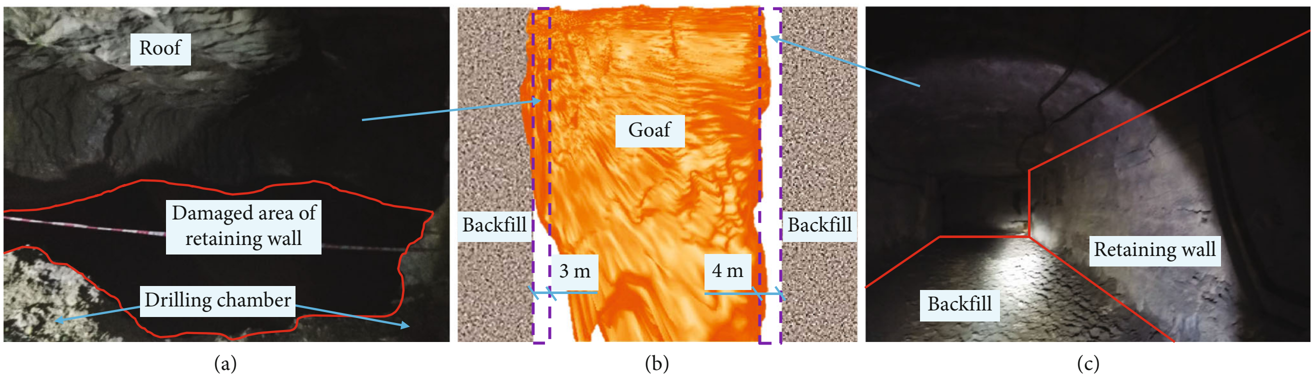

FIGURE 10: Shapes of goaf and retaining wall after the second-step mining: (a) retaining wall with a thickness of 3 m collapsed, (b) scanning results of the goaf, and (c) retaining wall with a thickness of 4 m remained fairly stable without collapsing.

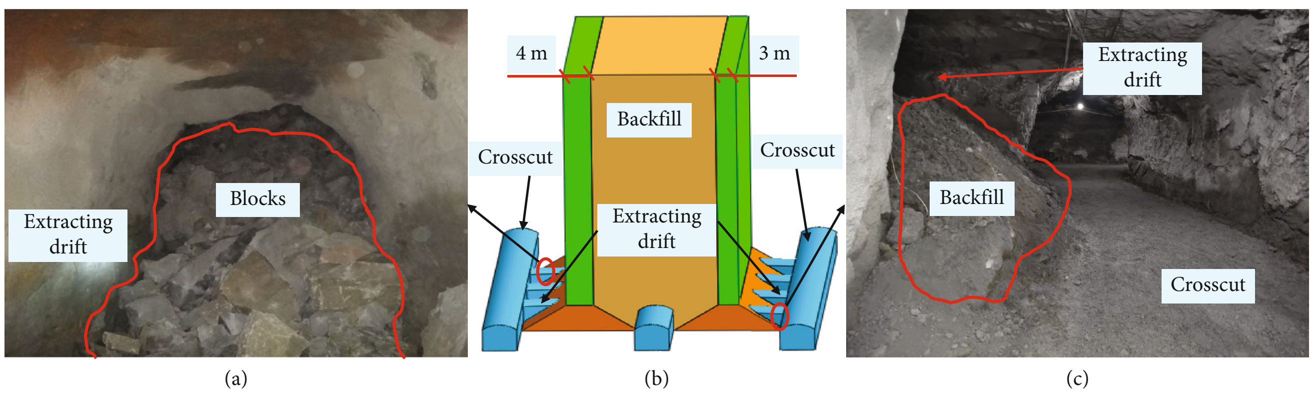

FIGURE 11: Reaction of retaining walls with different thicknesses after the second-step mining: (a) blocks from extracting drift, (b) stope bottom structure, and (c) filling mass from extracting drift due to collapsion of retaining wall.

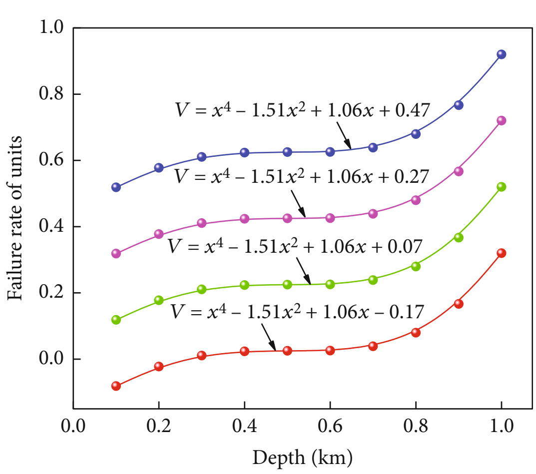

FIGURE 12: Curves after increasing c.

applied in this study only takes the essence of the catastrophe theory to study the nonlinear evolution of the unit failure rate of retaining wall, which should be widely utilized.

5.2. Effect of c in the Catastrophe Model. The standard expression of catastrophe model (1) is a quartic equation, which does not include a constant. Generally, regardless of the way of derivation, there must be a constant c in the final established standard expression of catastrophe model, and equation (1) will become

$$y(x) = x^4 + ax^2 + bx + c. \tag{11}$$

Obviously, the catastrophe models derived in actual studies are not standard forms. However, when equation (3) is regarded as the criterion for deriving the catastrophe model, the equilibrium equation obtained is the same as equation (2) by deriving equation (11) and making it equal to 0. In other words, the criterion of the catastrophe model is the same regardless of whether there is constant c in formula (11). It can be seen that according to the catastrophe theory, the constant c has nothing to do with the change of system state.

In fact, although the constant c is not related to the control variables a and b, as well as the state variable x, the magnitude of c affects y, namely, the unit failure rate of the retaining wall. When c increases, the unit failure rate of the retaining wall increases, and when it reaches a certain level, the retaining wall is bound to be destabilized.

Taking the curve of $D = 10$ m in Figure 9 as an example, the equation is

$$y(x) = x^4 - 1.51x^2 + 1.06x - 0.17. \tag{12}$$

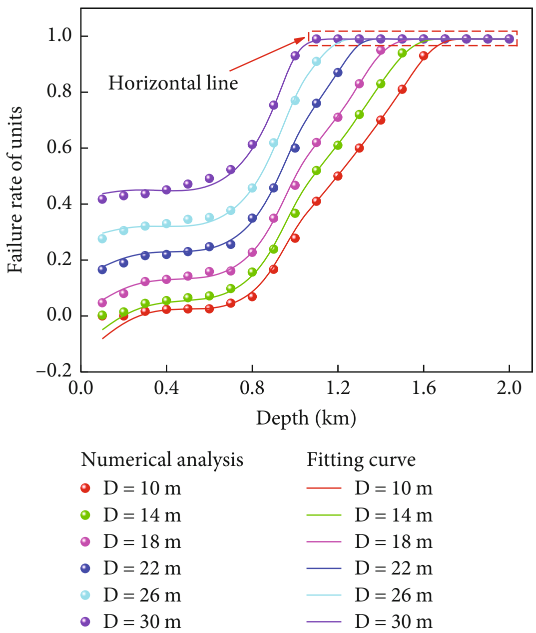

Figure 13: Fitted curve for mining depths over 1000 m.

It is obvious that the retaining wall remains stable because $\Delta > 0$ in equation (12). According to the catastrophe theory, Δ has nothing to do with c; no matter how c changes, as long as $\Delta > 0$, the retaining wall will remain stable. However, from the point of view of numerical analysis, assuming that the value of c continues to increase, the curve will continue to rise from the bottom to the top, and the curve will become the shape shown in Figure 12. As a result, the unit failure rate of the retaining wall tends to 100%, and retaining wall will eventually be penetrated by the plastic zone, and destabilization is about to occur. Therefore, it is not difficult to find that the constant c seems to have an effect on the state change of the system, which is different from the result produced by the catastrophe theory. Obviously, whether c plays a role in the process of catastrophic instability of retaining wall needs further in-depth study.

5.3. Limitation of Mining Depth. In fact, although the use of numerical simulation analysis to fit the standard expression of catastrophe model greatly simplifies the complex formula derivation, it also has its own limitations. Theoretically, the unit failure rate of the retaining wall increases with the increase of mining depth, but its upper limit is 100%, which does not increase with the increase of mining depth. As a result, when the unit failure rate of retaining wall reaches close to 100%, the failure rate will no longer increase even if the mining depth continues to increase. The curve enters the postpeak stage, where the curve has been transformed into a horizontal line, as shown in Figure 13.

The dashed frame in Figure 13 is the extension of the curve with its $D = 30$ m, and the fitted curve can be divided into two stages, prepeak and postpeak, with the mining depth of 1000 m as the dividing line. In the prepeak stage, the standard form of the fitted catastrophe model (1) obtained by fitting is so good that it is advisable to use catastrophe theory to analyze the change of retaining wall state. In contrast, the curve of the postpeak phase is approximately a horizontal straight line, which cannot be fitted with the standard form of the catastrophe model (1). Undoubtedly, the catastrophe theory should not be applied mechanically to study the change of the retaining wall state at this stage. Similar patterns can be found in the other curves in Figure 13, where the dividing line between the two stages before and after the peak only is not in the same position. It can be seen that the coupling method of numerical simulation and catastrophe theory to study the stability of the retaining wall is limited by the mining depth, and the closer the failure rate of the retaining wall unit is to the peak, the greater the deviation of the analysis by this method.

6. Conclusion

(1) The retaining wall of the stope is regarded as the research object, and the criterion for the instability and failure of retaining wall is established by combining catastrophe theory with numerical simulation. The unit failure rate of retaining wall increases by continuously decreasing the thickness of retaining wall until the instability and failure occurs in the retaining wall. Then, the critical thickness of retaining wall can be accurately calculated. This provides a new method for the study of retaining wall stability

(2) The change of the retaining wall is studied by reducing the same thickness of the retaining wall every time. In the process of reducing the thickness from 8 m to 2 m, the position of the fitting curves continues to move up. Moreover, with the reduction of thickness, a increases but Δ decreases and tends to be negative. When the thickness of retaining wall is 3 m, Δ will be smaller than 0, which means that the retaining wall becomes unstable

(3) The increase of stope span will have an effect on the retaining wall stability. For the retaining wall with a thickness of 4 m, the catastrophic instability occurs when its span increases to 22 m. The critical spans are 15 m, 18 m, and 28 m when the thicknesses of retaining wall are 2 m, 3 m, and 5 m, respectively. However, when the retaining wall is thicker than 5 m, the retaining wall will be stable as long as the span is smaller than 30 m. It can be seen that the thicker the retaining wall is, the better the adaptability of the stope is to the span

(4) The application test of retaining wall was carried out in stope #2 of the copper mine to verify the research results. According to the field observation and the scanning results of the goaf, it can be found that catastrophic instability is bound to occur in the retaining wall with a thickness of 3 m, but the retaining wall with a thickness of 4 m maintains stable, which can provide a long-lasting and stable protective barrier for the backfill in the first-step stope

Data Availability

The data used to support the findings of this study are available from the corresponding author upon request.

Conflicts of Interest

The authors declare that there is no conflict of interest regarding the publication of this paper.

Acknowledgments

This work was supported by National Key Research and Development Program of China (No. 2017YFC0804601) and National Natural Science Foundation of China (No. 51664018). The authors are very grateful for the financial contributions and convey their appreciation to the organizations for supporting this basic research.

References

[1] S. Jian, L. Xin, and R. Ting, "Overburden stability of an inclined backfill stope in the context of the nonlinear elastic mechanical properties of the backfill body," *Environmental Earth Sciences*, vol. 78, no. 24, 2019.

[2] Y. N. Shaposhnik, A. I. Konurin, S. A. Neverov, O. M. Usol't-seva, and S. N. Shaposhnik, "Validation of friction-anchored rock bolt supports for underground excavations in backfill," *Journal of Mining Science*, vol. 57, no. 5, pp. 775–786, 2021.

[3] J. Wang, D. P. Qiao, R. S. Han, G. T. Li, and J. C. Xie, "Strength model of cemented backfill in subsequent filling at the stage of open stope and its application," *Rock and Soil Mechanics*, vol. 40, pp. 1105–1112, 2019.

[4] Y. I. Rubchevsky, *Geomechanical Substantiation of Mine Support Systems for Stopes in Backfill in Yakovlevsky Mine*, Cand. Tech. Sci. Dissertation, Saint-Petersburg: SPGU, 2016.

[5] T. Belem and M. Benzaazoua, "Design and application of underground mine paste backfill technology," *Geotechnical and Geological Engineering*, vol. 26, no. 2, pp. 147–174, 2008.

[6] D. Ma, J. X. Zhang, H. Y. Duan et al., "Reutilization of gangue wastes in underground backfilling mining: overburden aquifer protection," *Chemosphere*, vol. 264, Part 1, article 128400, 2021.

[7] D. Ma, H. Y. Duan, and J. X. Zhang, "Solid grain migration on hydraulic properties of fault rocks in underground mining tunnel: radial seepage experiments and verification of permeability prediction," *Tunnelling and Underground Space Technology*, vol. 126, article 104525, 2022.

[8] J. W. Bai, B. Q. Cui, and T. Y. Qi, "Fundamental theory for rick strata control of key pillar-side backfilling," *Journal of China Coal Society*, vol. 46, pp. 424–438, 2021.

[9] S. M. Chen, A. X. Wu, Y. M. Wang, and X. Chen, "Analysis of influencing factors of pillar stability and its application in deep mining," *Journal of Central South University (Science and Technology)*, vol. 49, pp. 2050–2057, 2018.

[10] T. Hauquin, Y. Gunzburger, and O. Deck, "Predicting pillar burst by an explicit modelling of kinetic energy," *International Journal of Rock Mechanics and Mining Sciences*, vol. 107, pp. 159–171, 2018.

[11] S. Y. Wang, S. W. Sloan, M. L. Huang, and C. A. Tang, "Numerical study of failure mechanism of serial and parallel rock pillars," *Rock Mechanics and Rock Engineering*, vol. 44, no. 2, pp. 179–198, 2011.

[12] Z. L. Zhou, L. Chen, Y. Zhao, T. B. Zhao, and X. M. Du, "Experimental and numerical investigation on the bearing and failure mechanism of multiple pillars under overburden," *Rock Mechanics and Rock Engineering*, vol. 50, no. 4, pp. 995–1010, 2017.

[13] L. Li and M. Aubertin, "A modified solution to assess the required strength of exposed backfill in mine stopes," *Canadian Geotechnical Journal*, vol. 49, no. 8, pp. 994–1002, 2012.

[14] S. C. Wu, T. Li, H. Y. Cheng, X. Q. Zhang, and Z. Q. Zhao, "Mechanical response and stability of horizontal pillar size evolution in high stress environment," *Journal of Central South University (Science and Technology)*, vol. 52, pp. 1027–1039, 2021.

[15] L. C. Jiang and Y. D. Wang, "Comprehensive safety factor of residual mining pillar under complex loads," *Journal of Central South University (Science and Technology)*, vol. 49, pp. 1512–1518, 2018.

[16] J. X. Fu, W. D. Song, and Y. Y. Tan, "Study on influence of overlapping rate of double layer gobs on stability of isolation roof and its mechanical model," *Journal of Mining and Safety Engineering*, vol. 35, pp. 59–63, 2018.

[17] X. Z. Shi, W. Y. Ke, Y. G. Gou, X. F. Huo, and Z. H. Kan, "Optimization of strip pillar size in upper chamber of long-span stope," *Journal of Mining and Safety Engineering*, vol. 37, pp. 1084–1093, 2020.

[18] S. Bala Padmaja, G. V. Narasimha Reddy, and E. Saibaba Reddy, "A catastrophe theory for planar sliding slope," in *Soil Dynamics and Earthquake Geotechnical Engineering*, B. Adimoolam and S. Banerjee, Eds., vol. 15 of Lecture Notes in Civil Engineering, Springer, Singapore, 2019.

[19] Z. Z. Cao and Y. J. Zhou, "Research on instability mechanism and type of ore pillar based on the fold catastrophe theory," *Computer Modeling in Engineering & Sciences*, vol. 113, pp. 275–293, 2017.

[20] D. M. Wang, E. Y. Wang, X. J. Feng et al., "Triaxial creep damage–catastrophe instability characteristics and a nonlinear constitutive model of gas-bearing coal," *Bulletin of Engineering Geology and the Environment*, vol. 81, no. 10, pp. 437–454, 2022.

[21] L. Li and M. Aubetin, "An improved method to assess the required strength of cemented backfill in underground stopes with an open face," *International Journal of Mining Science and Technology*, vol. 24, no. 4, pp. 549–558, 2014.

[22] Q. Chen, H. G. Yan, and H. L. Chang, "Study on rock burst prediction of deep buried tunnel based on cusp catastrophe theory," *Geotechnical and Geological Engineering*, vol. 39, pp. 1101–1115, 2021.

[23] F. C. Zhou, H. M. Tang, C. Song, F. Lin, and S. Chao, "Research on the damage-catastrophe mechanism of a tower-column unstable rock mass with compressed-fracture slumping mode under multi-factor couplings," *Geotechnical and Geological Engineering*, vol. 26, pp. 1007–1034, 2022.

[24] K. H. Han, J. W. W. Ju, H. Kong, and M. S. Wang, "Functional catastrophe analysis of progressive failures for deep tunnel roof considering variable dilatancy angle and detaching velocity," *Rock Mechanics and Rock Engineering*, vol. 52, no. 10, pp. 3987–3997, 2019.

[25] X. T. Liu, C. X. Chen, X. M. Liu, and K. Z. Xia, "Analysis of catastrophic instability of roof-rib pillar support system under backfill mining," *Rock and Soil Mechanics*, vol. 42, pp. 2461–2471, 2021.

[26] K. Z. Xia, X. M. Liu, C. X. Chen, Y. F. Song, Z. Ou, and Y. Long, “Analysis of mechanism of bedding rock slope instability with catastrophe theory,” *Rock and Soil Mechanics*, vol. 36, pp. 477–486, 2015.

[27] C. L. Mu, X. J. Pei, J. F. Lu, Z. Pei, and Z. H. Xi, “Study on the instability criterion of layered rock mass failure based on the cusp catastrophe theory,” *Journal of China Coal Society*, vol. 42, pp. 1429–1435, 2017.

[28] S. Sadeghfam, Y. Hassanzadeh, A. A. Nadiri, and M. Zarghami, “Localization of groundwater vulnerability assessment using catastrophe theory,” *Water Resources Management*, vol. 30, pp. 4585–4601, 2016.

[29] J. H. Guo, C. Y. She, H. B. Liu, and S. Cui, “Rock mechanical properties and wellbore stability of fractured dolomite formations,” *ACS Omega*, vol. 8, no. 38, pp. 35152–35166, 2023.

[30] H. Liu, S. Cui, Y. Meng, Z. Han, and M. Yang, “Study on rock mechanical properties and wellbore stability of fractured carbonate formation based on fractal geometry,” *ACS Omega*, vol. 7, no. 47, pp. 43022–43035, 2022.

[31] I. G. Raftoyiannis, T. G. Constantakopoulos, G. T. Michaltsos, and A. N. Kounadis, “Dynamic buckling of a simple geometrically imperfect frame using catastrophe theory,” *International Journal of Mechanical Sciences*, vol. 48, no. 10, pp. 1021–1030, 2006.

[32] X. B. Xie, R. N. Deng, X. J. Dong, and T. Y. Tian, “Stability of goaf group system based on catastrophe theory and rheological theory,” *Rock and Soil Mechanics*, vol. 39, pp. 1963–1972, 2018.

[33] X. R. Wang, K. Guan, T. H. Yang, and X. G. Liu, “Instability mechanism of pillar burst in asymmetric mining based on cusp catastrophe model,” *Rock Mechanics and Rock Engineering*, vol. 54, no. 3, pp. 1463–1479, 2021.

[34] Z. H. Zhou, Z. H. Chen, L. F. Zhang, G. Q. Nian, J. M. Wang, and X. F. Jiao, “Energy principle-based catastrophe study of slope stability in open-pit excavation,” *Rock and Soil Mechanics*, vol. 40, pp. 4881–4889, 2019.

[35] Z. H. Zhou, Z. H. Chen, M. Bao, G. Q. Nian, and W. Zhang, “Stability of rock slope with bedding intermittent joints based on catastrophe theory,” *Journal of China Coal Society*, vol. 45, pp. 161–172, 2020.

[36] Z. H. Zhao, J. Y. Xu, J. H. Yuan, W. Y. Chang, and G. H. Guo, “Investigation of cusp catastrophe model of rock slope instability with general constitutive equations,” *Bulletin of Engineering Geology and the Environment*, vol. 80, no. 1, pp. 303–315, 2021.

[37] H. Xu, Y. M. Wang, A. X. Wu, F. F. Li, and W. H. Gao, “A computational model of safe thickness of roof under filling body based on cusp catastrophe theory,” *Chinese Journal of Rock Mechanics and Engineering*, vol. 36, pp. 579–586, 2017.

[38] X. D. Xu, Y. J. Zhou, and S. Pang, “Analysis of catastrophic instability of plastic supporting system in old goaf of gypsum mine,” *Chinese Journal of Rock Mechanics and Engineering*, vol. 37, pp. 2548–2555, 2018.

[39] D. F. Yang, Z. H. Chen, Q. F. Hong, J. Y. Xi, Q. F. Hong, and S. S. Zhang, “Catastrophic analysis of support crushing disasters while roof cutting in shallow seam mining,” *Journal of Mining and Safety Engineering*, vol. 33, pp. 122–127, 2016.

[40] K. Z. Xia, C. X. Chen, X. T. Liu, M. X. Liu, J. H. Yuan, and S. Dang, “Assessing the stability of high-level pillars in deeply-buried metal mines stabilized using cemented backfill,” *International Journal of Rock Mechanics and Mining Sciences*, vol. 170, article 105489, 2023.

[41] Y. L. Zhao, Q. H. Wu, W. J. Wang, W. Wan, and F. J. Zhao, “Strength reduction method to study stability of goaf overlapping roof based on catastrophe theory,” *Chinese Journal of Rock Mechanics and Engineering*, vol. 29, pp. 1424–1434, 2010.

[42] X. D. Zhao, X. Zhou, Y. F. Zhao, and W. L. Yu, “Research status and progress of prevention and control of mining disasters in deep metal mines,” *Journal of Central South University (Science and Technology)*, vol. 52, pp. 2522–2538, 2021.